

Off-easy-plane antiferromagnetic spin canting in coupled FePt/NiO bilayer structure with perpendicular exchange bias

Tenghua Gao,¹ Nobuhide Itokawa,¹ Jian Wang,² Youxing Yu,³ Takashi Harumoto,¹ Yoshio Nakamura,¹ and Ji Shi^{1,*}

¹*Department of Metallurgy and Ceramics Science, Tokyo Institute of Technology, 2-12-1 Oh-okayama, Meguro-ku, Tokyo 152-8552, Japan*

²*National Institute of Materials Science (NIMS), Sengen 1-2-1, Tsukuba, Ibaraki 305-0047, Japan*

³*School of Materials Science and Engineering, Beihang University, Beijing 100191, People's Republic of China*

(Received 23 March 2016; revised manuscript received 26 May 2016; published 10 August 2016)

We report on the investigation of perpendicular exchange bias in FePt(001)/NiO($\bar{1}\bar{1}\bar{1}$) orthogonal exchange couple with FePt partially $L1_0$ ordered. From initial magnetization curve measurement and magnetic domain imaging, we find that, for the as-grown bilayer structure, the FePt layer experiences a small-angle magnetization rotation when it is magnetized near to saturation in film normal direction. After field cooling, the bilayer structure shows a significant enhancement of perpendicular magnetic anisotropy, indicating the field mediated coupling between the spins across the FePt/NiO interface. According to Koon's theoretical calculation on the basis of lowest energy ferromagnetic/antiferromagnetic coupling configuration for compensated spins at antiferromagnetic side, we consider slightly slanted Ni spins at the interface off the ($\bar{1}\bar{1}\bar{1}$) easy plane can stabilize the spin coupling between FePt and NiO and result in the observed exchange bias in this paper. This consideration was further confirmed by stripe domain width calculation.

DOI: [10.1103/PhysRevB.94.054412](https://doi.org/10.1103/PhysRevB.94.054412)

The interface interaction between ferromagnetic (FM) and antiferromagnetic (AFM) layers leads to the well-known exchange bias effect [1]. Although intensive research attention has been paid to explain the mechanism for this phenomenon since its discovery half a century ago [2], the origin of exchange bias is still under debate. It firstly assumes a perfectly uncompensated AFM interface with collinear FM/AFM exchange coupling at the interface [3], and Mauri *et al.* pointed out that exchange bias occurs due to the formation of AFM planar domain wall as the FM magnetization is reversed [4]. The reason for the large discrepancy between the actual and predicted values has been further studied with the recognition that effects such as coupling frustration at the FM/AFM interface [5,6], constituted only a small percentage of uncompensated AFM spins in the real cases [7,8], or a partial wall formed in the soft FM layer at the interface [9]. Recently, orthogonal FM/AFM exchange coupling was realized in Fe/CoO [10,11] and Fe/NiO [12,13] structures as confirmed by an AFM spin switching study using x-ray magnetic linear dichroism (XMLD), and this “spin flop” coupling has already been proposed from theoretical calculation for a compensated AFM interface [5,14]. Due to the absence of unidirectional anisotropy [15], the mechanism of exchange bias in such a coupling system can not be explained by Mauri's model. While based on the results of numerical simulation, the AFM spins should deviate slightly away from the easy axis direction (i.e., the angle between FM and AFM spin is not exact 90°) due to the competing AFM exchange between the two sublattices and the ferromagnet [5,14,16]. However, to our knowledge, this small deviating angle has rarely been considered or proved in a real orthogonal FM/AFM coupling system. From recent studies, it is known that, for the application of exchange bias effect in advanced spintronic devices, perpendicular exchange bias (PEB) is much more desirable [17–19]. The out-of-plane alignment of FM spins can also facilitate the theoretical study

of exchange bias, especially how the AFM spins affect the FM spin alignment during the magnetization process in domain imaging experiments [8,20].

In this paper, we present the study of perpendicular-exchange-biased FePt/NiO bilayers on MgO(001) single crystal substrate in which the $L1_0$ FePt exhibits strong perpendicular magnetic anisotropy. In this structure, any deviation of Fe spins from the normal direction may be considered to be caused by FM/AFM coupling. On the other hand, the interfacial spin configuration of NiO can be “visualized” through the magnetization of FePt. This means our structure and experimental approach offer a way to study the interfacial spin structure between the FM and AFM layers. By comparing the FePt single layer and FePt/NiO bilayers before and after perpendicular field cooling (FC), we observed that only the bilayer before FC experiences a small-angle magnetization rotation as it is magnetized near to saturation in normal direction. Meanwhile, after FC, the bilayer shows a significant enhancement of perpendicular magnetic anisotropy. These findings provide experimental evidence that, for FM/AFM orthogonal coupling, the angle between FM and AFM spin is not exactly 90° as predicted by theoretical calculation [5,14], which is expected to induce a unidirectional anisotropy in the FM layer after FC.

MgO(001) single crystal substrates were cleaned in ultrasonic baths of acetone and methyl alcohol, and surface thermal cleaning was implemented in an ultrahigh vacuum system by annealing at 840 K for 90 min. Then samples of the FePt(2.5 nm) single layer and FePt(2.5 nm)/NiO(21 nm) bilayers were grown epitaxially on MgO(001) substrates. The 2.5 nm thick FePt layer was grown by dc magnetron sputtering on top of MgO(001) substrate held at 620 K, followed by an *in situ* annealing at 840 K for 3 h to induce the $L1_0$ ordering. Our two-step preparation method is expected to prevent the island growth of FePt at high substrate temperatures [21]. For the FePt/NiO bilayers, a NiO(21 nm) layer was subsequently deposited on top of the FePt layer at 500 K by dc reactive sputtering in a mixture atmosphere of Ar and O₂ gases

*shi.j.aa@m.titech.ac.jp

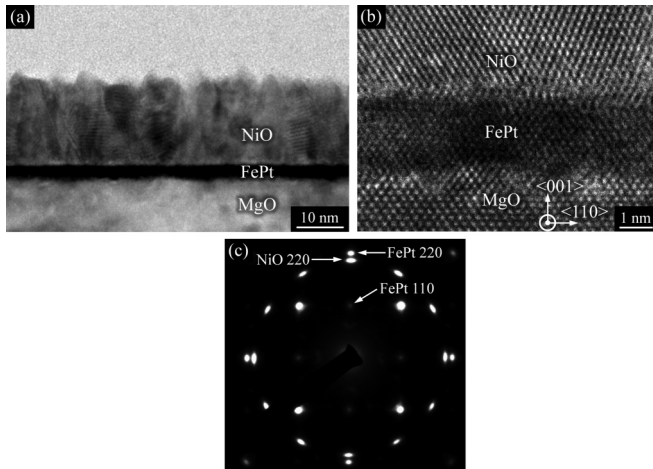


FIG. 1. (a) Low magnification TEM micrograph of cross-sectional FePt/NiO bilayer structure. (b) Corresponding high resolution TEM image taken with MgO[110] as zone axis. (c) Plan-view selected-area electron diffraction pattern of FePt/NiO bilayer structure taken with FePt [001] as zone axis.

(2% O₂). The structure of the FePt single layer and FePt/NiO bilayers was characterized by x-ray diffraction (XRD) and x-ray reflectivity (XRR). Microstructural characterization was carried out by transmission electron microscopy (TEM). The magnetic properties were characterized by superconducting quantum interference device (SQUID) magnetometer. The

magnetic domain imaging was performed at 300 K by magnetic force microscopy (MFM).

Figure 1(a) shows a low magnification cross-section TEM image of the FePt(2.5 nm)/NiO(21 nm) bilayer structure, which reveals that a continuous FePt layer with sharp FePt/NiO interface was formed. The order parameter of FePt calculated from XRD for the FePt single layer and FePt/NiO bilayer structures is 0.51 and 0.53, respectively, indicating that these two systems should possess the same uniaxial magnetic anisotropy (K_u) [22]. The interface condition was further confirmed by the corresponding high-resolution TEM image, and there is no sight of interface diffusion or Fe oxidation as shown in Fig. 1(b). Both the electron diffraction and XRD results show that NiO(111) has been epitaxially grown on FePt(001). From plan-view electron diffraction pattern taken with FePt[001] as the zone axis shown in Fig. 2(c), the epitaxial relationship between FePt and NiO is established: $(001)[1\bar{1}0]_{\text{FePt}} \parallel (111)[1\bar{1}0]_{\text{NiO}}$. In the film plane, NiO has two epitaxial orientations with the sixfold $\{110\}$ rotated by 30° (or 90°) against each other. This epitaxial relationship was also confirmed by in-plane XRD and φ scan XRD. In an epitaxial thin film, the anisotropy of NiO is dominated by the magnetoelastic effect resulting from epitaxial strain [12,23]. While at the FePt/NiO interface in our sample, the epitaxial misfits along NiO [112] and $[1\bar{1}0]$ axes obtained from in-plane XRD are -6.7% and +7.5%, respectively. With the consideration of the recently reported FePt(001)/CoO(111) system, such an in-plane anisotropic strain in CoO leads to the out-of-plane $[\bar{1}\bar{1}1]$ stacking direction favorable, consequently

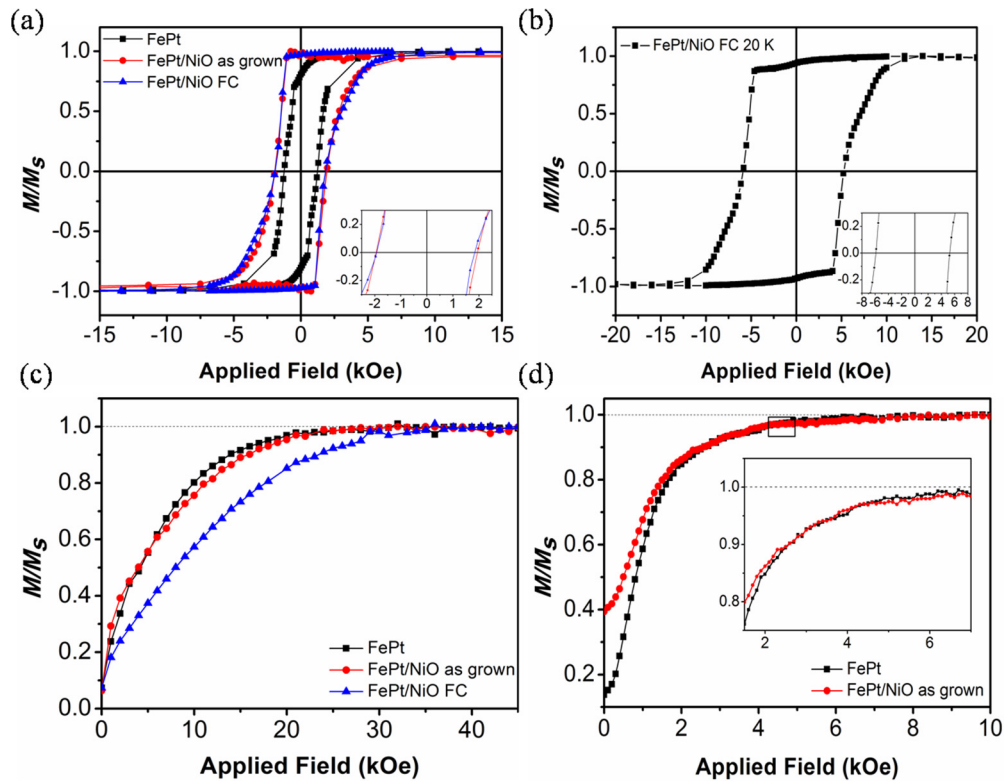


FIG. 2. Magnetic properties of FePt single layer and FePt/NiO bilayer structures. (a) Perpendicular hysteresis loops measured at 300 K for FePt single layer, and bilayers as grown and after FC. (b) Perpendicular hysteresis loop for bilayers measured at 20 K after FC. The inset shows the enlarged loops around coercive field for bilayers. (c) Initial magnetization curves at 300 K measured along in-plane direction. (d) Perpendicular initial magnetization curves at 300 K. The inset in panel (d) shows the enlarged curves around cross point.

forming a fully compensated AFM interface [24]. This provides a useful reference for our FePt/NiO structure. Since the Ni spins are aligned along $\langle 112 \rangle$ directions within $\{111\}$ planes in the bulk [25,26], it is reasonable to expect that the initial AFM spin alignment at FePt(001)/NiO($\bar{1}\bar{1}1$) interface will be in the film plane containing fully compensated spins.

Figures 2(a) and 2(b) show the perpendicular hysteresis loops of the FePt single layer and FePt/NiO bilayers before and after FC. Field cooling treatment for the bilayer structure was performed in a low vacuum (1.33 Pa) with a perpendicular magnetic field of 5 kOe from 530 K (above the Néel temperature 523 K of NiO) to room temperature because, for the Fe/NiO bilayer structure, the XPS spectra do not show a significant change in chemical state of Fe up to a heat treatment temperature of 540 K [27], while during the FePt ordering, it tends to form a Pt terminated (001) surface [28,29]. Thus, the magnetic properties of FePt are considered not affected by our FC treatment [24]. From perpendicular hysteresis loops, we can observe that all three samples possess strong perpendicular magnetic anisotropy. The resulting hysteresis loop after FC shows an exchange bias field of -41 Oe at 300 K and increases to -301 Oe at 20 K [Fig 2(b)]. Figure 2(c) shows the initial in-plane magnetization curves obtained at 300 K. The greatly increased saturation field for the bilayers after FC indicates that the Fe spins become more stable along the film normal direction. In order to clarify the influence of NiO on the perpendicular magnetization process, the perpendicular initial magnetization curves for the as-grown FePt single layer and FePt/NiO bilayers were measured at 300 K as shown in Fig. 2(d). The nonzero magnetization at the starting point is because a 200 Oe field was applied to center the sample position in the SQUID chamber before the measurement. At the first stage, the magnetization of the FePt/NiO bilayers rapidly increases. However, when it is close to saturation, the magnetization becomes harder and finally intersects with the magnetization curve of the FePt film. This observation suggests that the deposition of NiO induces a pinning effect to the magnetization of the FePt layer in the as-grown bilayer structure as it is magnetized close to the saturation.

To further elucidate the impact of NiO on the FePt layer, we imaged magnetic domain structures in different remanent states. Figure 3 shows MFM images of the FePt single layer and FePt/NiO bilayers that were subjected to different field sequences. Since the MFM images are adjusted within the same contrast range, the contrast level bar located near Fig. 3(h) is applicable to all the images. For the as-grown structures [see Figs. 3(a) and 3(b)], both samples exhibit stripe domains. The increase of the domain width for the bilayer structure is due to the induced anisotropy from FM/AFM coupling, which will be discussed below. After magnetizing along normal direction with 5 kOe applied field, only small unreversed domains are observable for the FePt single layer [see circles in Fig. 3(c)], while for bilayers, a faint stray field contrast is visible, indicating the existence of FM magnetization fluctuation slightly off the film normal direction [Fig. 3(d)]. In the case of the bilayer structure after FC, the FM layer was saturated and a single domain structure was formed as shown in Fig. 3(e). Subsequently applying a 15 kOe in-plane field to partially demagnetize films, inhomogeneous nucleation bubble domains in coexistence with irregular stripe

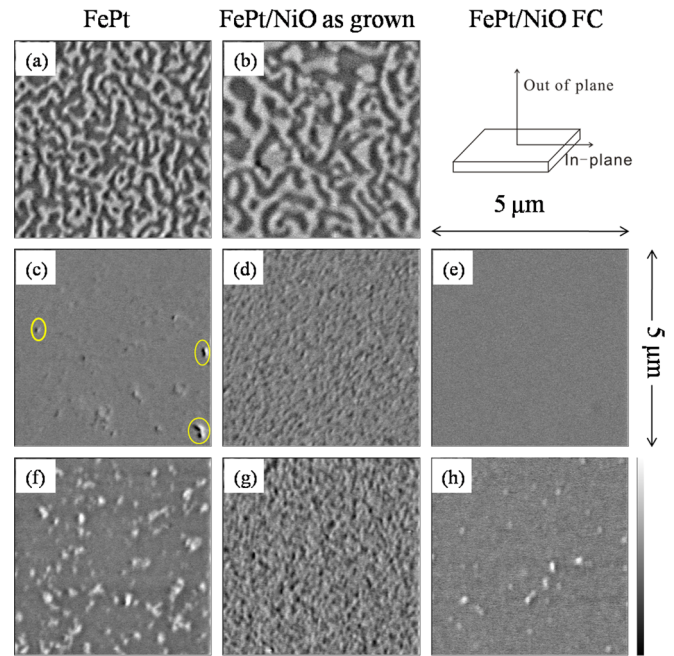


FIG. 3. Magnetic domain structures in FePt single layer and FePt/NiO bilayers for different remanence. The MFM measurements were performed at 300 K. MFM images of (a) as-grown FePt single layer and (b) bilayers. MFM images of (c) FePt single layer and (d) bilayers after magnetizing in film normal direction with a field of 5 kOe. (e) MFM image of bilayer structure after perpendicular FC with 5 kOe external magnetic field. A partially demagnetizing field was applied along in-plane direction with a field of 15 kOe to (c)–(e). The corresponding domain images were recorded as (f)–(h).

domains appears in the FePt single layer [Fig. 3(f)]. However, for the bilayers after FC, only bubble domains are observable as shown in Fig. 3(h). Interestingly, for the as-grown bilayers, the faint contrast is enhanced [Fig. 3(g)]. From the MFM results presented above, the following conclusions can be drawn: (i) During the magnetization process, compared with the structure of stripes coexisting with bubble domains, the bubble domain structure is closer to the uniform domain structure (saturation) [30–32]. Therefore, an enhancement of perpendicular magnetic anisotropy for the FePt/NiO bilayer structure can be expected after FC. Such an enhancement was also reported in an orthogonal CoO/Ni coupling structure [33]. (ii) For the as-grown FePt/NiO bilayer structure, the faint stray field contrast observed in Figs. 3(d) and 3(g) reveals that a small angle rotation of magnetization is needed to be further magnetized to saturation. Both of these findings are in good agreement with the results from magnetization curves.

Here, we turn to discuss the AFM spin configuration at the FePt/NiO interface with the consideration of lowest energy coupling configuration proposed from numerical simulation [5,14,16]. The idea is that, at a fully compensated AFM interface, the coupling frustration results in the AFM spin deviation slightly from its easy axis to generate a net magnetic moment. Consequently, the FM spin aligns antiparallel to this induced moment, orienting perpendicular to the AFM easy axis. The resulting configuration is shown in the inset of Fig. 4. Figure 4 shows the out-of-plane canting of the AFM spins

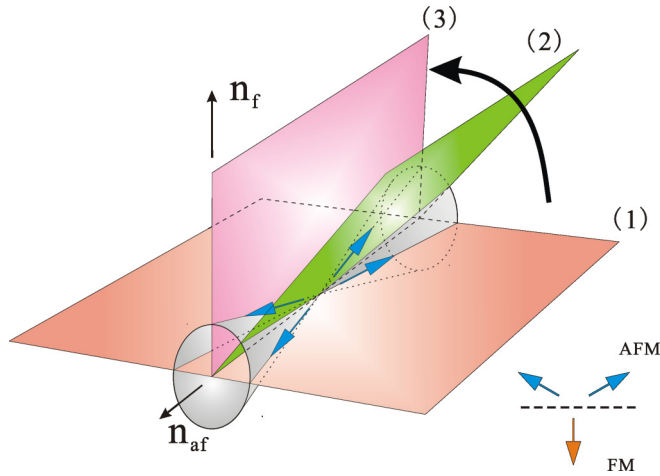


FIG. 4. Out-of-plane canting of AFM spins response to the adjacent FM spin. Blue arrows represent the AFM spins. Plane 1 and plane 3 represent the FM/AFM interface plane and normal plane, respectively. The inset shows lowest energy coupling configuration, where the deviation of FM/AFM coupling angle from 90° is somewhat exaggerated.

against the adjacent FM spin in different cases. In principle, owing to the large easy plane anisotropy, the Ni spins should be constrained in the (111) plane [34], forming a stable coupling configuration with the FM spin in plane (1). It is known that FC treatment results in the repopulation of AFM magnetic domains [35], and the alignment of AFM spins depends on the local FM order [25,36]. For the as-grown FePt/NiO bilayers, since the deposition temperature of NiO (500 K) is close to its Néel temperature ($T_N = 523$ K), following the deposition of NiO on top of FePt, the competition among strong perpendicular magnetic anisotropy of FePt, FM/AFM coupling, and NiO easy plane anisotropy leads to the out-of-plane canting of Ni spins. Consequently, the Ni spins lie in plane (2). Note that, due to the coupling between Fe spins and the resultant moment generated by Ni spin canting, the angle between planes (2) and (3) should be very small. In this configuration, an induced extra uniaxial anisotropy in the FePt layer can be expected, which is tilted slightly from the normal direction also in plane (2). As the Fe spins equally align either up or down to the interface during cooling, no unidirectional anisotropy can be obtained. However, for the bilayer structure after FC and during FC treatment, the magnetic field is large enough to confine the Fe spins in a certain direction along the film normal as confirmed by MFM measurement [Fig. 3(e)], giving rise to the Ni spins aligned in the normal plane [plane (3)] to form a lowest energy coupling configuration. It can be easily understood that this type of twist in the NiO layer will induce a unidirectional anisotropy in the FePt layer as well as an enhancement of perpendicular magnetic anisotropy.

In order to confirm the validity of our proposed mechanism above, the stripe domain width of FePt in the as-grown FePt single layer and FePt/NiO bilayers [Figs. 3(a) and 3(b)] was quantitatively analyzed. The formation of a magnetic domain is due to the competing energy of the magnetic exchange interaction, magnetocrystalline anisotropy, and magnetic dipolar interaction [37]. After NiO deposition, the exchange coupling

between NiO and the FePt layer can be regarded as an induced uniaxial anisotropy K_{sf} [33]. We assume that both induced K_{sf} and Fe spins are sufficiently close to the film normal direction. This assumption is quite reasonable because of the large perpendicular magnetic anisotropy of the FePt layer and high NiO deposition temperature. By using Yafet's model [38] and making the same approximation as Wu *et al.* [39], the total energy per unit area can be calculated from the magnetic domain structure. Subsequently, minimizing this energy in relation to the stripe domain width (L) and domain wall width (w), respectively, the L in the FePt layer can be written

$$L = \frac{5At\left(\frac{a_{\parallel}}{a_{\perp}}\right)\pi^2}{6\Omega_L} \cdot \frac{\exp\left\{\sqrt{\frac{At\left(\frac{a_{\parallel}}{a_{\perp}}\right)\pi^4}{4\Omega_L^2}(K_u t - \Omega_s + K_{sf}) + 1 + 1}}\right\}}{\sqrt{\frac{At\left(\frac{a_{\parallel}}{a_{\perp}}\right)\pi^4}{4\Omega_L^2}(K_u t - \Omega_s + K_{sf}) + 1 + 1}}, \quad (1)$$

where A and K_u stand for the exchange stiffness and uniaxial anisotropy constant of the FePt layer, respectively; t (2.5 nm) is the thickness of the FePt layer; a_{\parallel} (2.74 Å) and a_{\perp} (3.72 Å) are the FePt in-plane and out-of-plane lattice parameters, respectively; $\Omega_s = 2\pi M_0^2(2t/a_{\perp})a_{\parallel}$ is the short-range part of the dipolar interaction, where M_0 is the saturation magnetization of FePt; and $\Omega_L = 2\pi M_0^2(2t/a_{\perp})^2 a_{\parallel}^2$ is the long-range part of the dipolar interaction. Taking the value of $M_0 = 1100$ emu/cc, $A = 1 \times 10^6$ erg/cm [22] and adjusted $K_u = 1.4 \times 10^7$ erg cc $^{-1}$, we estimated L of FePt film as $L_{\text{FePt}} = 0.15 \mu\text{m}$. This value agrees well with the experimental value of $L_{\text{FePt}} = 0.10 - 0.17 \mu\text{m}$. Notice that the K_u value used in this calculation is slightly smaller than the reported experimental value (1.5×10^7 erg cc $^{-1}$) in Ref. [22], which is considered because of the magnetoelastic anisotropy resulting from the epitaxial strain in our ultrathin FePt layer. Introducing the anisotropy energy $K_{sf} = 0.12$ erg cm $^{-2}$ induced by the orthogonal coupling between Fe and NiO [13], the stripe domain with L of FePt in the FePt/NiO bilayer film was obtained $L_{\text{FePt/NiO}} = 0.17 \mu\text{m}$, which is very reasonable compared with the experimental value $L_{\text{FePt/NiO}} = 0.15 - 0.22 \mu\text{m}$.

In summary, we have studied the magnetic properties of the FePt/NiO bilayer structure grown on a MgO(001) single crystal substrate. The results have demonstrated that, for the as-grown bilayer structure, the out-of-plane canting of Ni spins induces an extra uniaxial anisotropy slightly off the film normal direction, giving rise to a small angle magnetization rotation when the magnetization is close to saturation along the film normal direction. After FC, the realignment of the Ni spins leads to the formation of lowest energy FM/AFM coupling in the normal plane as indicated by theoretical calculation, which induces a unidirectional anisotropy and an enhancement of perpendicular magnetic anisotropy. Furthermore, the calculation results of stripe domain width also support our proposed Ni spin canting mechanism. This finding will shed a particular light on the mechanism of exchange bias, especially for the recent intensively studied orthogonal FM/AFM coupling structures.

- [1] J. Nogués and I. Schuller, *J. Magn. Magn. Mater.* **192**, 203 (1999).
- [2] W. H. Meiklejohn and C. P. Bean, *Phys. Rev.* **102**, 1413 (1956).
- [3] W. H. Meiklejohn, *J. Appl. Phys.* **33**, 1328 (1962).
- [4] D. Mauri, H. C. Siegmann, P. S. Bagus, and E. Kay, *J. Appl. Phys.* **62**, 3047 (1987).
- [5] R. L. Stamps, *J. Phys. D* **33**, R247 (2000).
- [6] E. Jiménez, J. Camarero, J. Sort, J. Nogués, N. Mikuszeit, J. M. García-Martín, A. Hoffmann, B. Dieny, and R. Miranda, *Phys. Rev. B* **80**, 014415 (2009).
- [7] J. Camarero, Y. Pennec, J. Vogel, S. Pizzini, M. Cartier, F. Fettaf, F. Ernult, A. Tagliaferri, N. B. Brookes, and B. Dieny, *Phys. Rev. B* **65**, 140408(R) (2002).
- [8] P. Kappenberger, S. Martin, Y. Pellmont, H. J. Hug, J. B. Kortright, O. Hellwig, and Eric E. Fullerton, *Phys. Rev. Lett.* **91**, 267202 (2003).
- [9] R. Morales, Ali C. Basaran, J. E. Villegas, D. Navas, N. Soriano, B. Mora, C. Redondo, X. Battle, and Ivan K. Schuller, *Phys. Rev. Lett.* **114**, 097202 (2015).
- [10] J. Wu, J. S. Park, W. Kim, E. Arenholz, M. Liberati, A. Scholl, Y. Z. Wu, Chanyong Hwang, and Z. Q. Qiu, *Phys. Rev. Lett.* **104**, 217204 (2010).
- [11] Q. Li, G. Chen, T. P. Ma, J. Zhu, A. T. N'Diaye, L. Sun, T. Gu, Y. Huo, J. H. Liang, R. W. Li, C. Won, H. F. Ding, Z. Q. Qiu, and Y. Z. Wu, *Phys. Rev. B* **91**, 134428 (2015).
- [12] W. Kim, E. Jin, J. Wu, J. Park, E. Arenholz, A. Scholl, Chanyong Hwang, and Z. Q. Qiu, *Phys. Rev. B* **81**, 174416 (2010).
- [13] J. Li, M. Przybylski, F. Yildiz, X. L. Fu, and Y. Z. Wu, *Phys. Rev. B* **83**, 094436 (2011).
- [14] N. C. Koon, *Phys. Rev. Lett.* **78**, 4865 (1997).
- [15] J. Li, A. Tan, S. Ma, R. F. Yang, E. Arenholz, C. Hwang, and Z. Q. Qiu, *Phys. Rev. Lett.* **113**, 147207 (2014).
- [16] M. D. Stiles and R. D. McMichael, *Phys. Rev. B* **59**, 3722 (1999).
- [17] S. Mangin, D. Ravelosona, J. A. Katine, M. J. Carey, B. D. Terris, and E. E. Fullerton, *Nat. Mater.* **5**, 210 (2006).
- [18] S. Ikeda, K. Miura, H. Yamamoto, K. Mizunuma, H. D. Gan, M. Endo, S. Kanai, J. Hayakawa, F. Matsukaru, and H. Ohno, *Nat. Mater.* **9**, 721 (2010).
- [19] Y. Shiratsuchi, H. Noutomi, H. Oikawa, T. Nakamura, M. Suzuki, T. Fujita, K. Arakawa, Y. Takechi, H. Mori, T. Kinoshita, M. Yamamoto, and R. Nakatani, *Phys. Rev. Lett.* **109**, 077202 (2012).
- [20] I. Schmid, M. A. Marioni, P. Kappenberger, S. Romer, M. Parlinska-Wojtan, H. J. Hug, O. Hellwig, M. J. Carey, and E. E. Fullerton, *Phys. Rev. Lett.* **105**, 197201 (2010).
- [21] Y. K. Takahashi, K. Hono, T. Shima, and K. Takanashi, *J. Magn. Magn. Mater.* **267**, 248 (2003).
- [22] S. Okamoto, N. Kikuchi, O. Kitakami, T. Miyazaki, Y. Shimada, and K. Fukamichi, *Phys. Rev. B* **66**, 024413 (2002).
- [23] I. P. Krug, F. U. Hillebrecht, M. W. Haverkort, A. Tanaka, L. H. Tjeng, H. Gomonay, A. Fraile-Rodríguez, F. Nolting, S. Cramm, and C. M. Schneider, *Phys. Rev. B* **78**, 064427 (2008).
- [24] A. D. Lamirand, M. M. Soares, A. Y. Ramos, H. C. N. Tolentino, M. De Santis, J. C. Cezar, A. de Siervo, and M. Jamet, *Phys. Rev. B* **88**, 140401(R) (2013).
- [25] H. Ohldag, A. Scholl, F. Nolting, S. Anders, F. U. Hillebrecht, and J. Stöhr, *Phys. Rev. Lett.* **86**, 2878 (2001).
- [26] D. Alders, L. H. Tjeng, F. C. Voogt, T. Hibma, G. A. Sawatzky, C. T. Chen, J. Vogel, M. Sacchi, and S. Iacobucci, *Phys. Rev. B* **57**, 11623 (1998).
- [27] P. Luches, S. Benedetti, A. di Bona, and S. Valeri, *Phys. Rev. B* **81**, 054431 (2010).
- [28] M. Müller and K. n Albe, *Phys. Rev. B* **72**, 094203 (2005).
- [29] L. Han, U. Wiedwald, B. Kuerbanjiang, and P. Ziemann, *Nanotechnology* **20**, 285706 (2009).
- [30] J. Wu, J. Choi, C. Won, Y. Z. Wu, A. Scholl, A. Doran, C. Hwang, and Z. Q. Qiu, *Phys. Rev. B* **79**, 014429 (2009).
- [31] N. Saratz, A. Lichtenberger, O. Portmann, U. Ramsperger, A. Vindigni, and D. Pescia, *Phys. Rev. Lett.* **104**, 077203 (2010).
- [32] J. Jeong, I. Yang, J. Yang, O. E. Ayala-Valenzuela, D. Wulferding, J.-S. Zhou, J. B. Goodenough, A. de Lozanne, J. F. Mitchell, N. Leon, R. Movshovich, Y. Hee Jeong, H. Woong Yeom, and J. Kim, *Phys. Rev. B* **92**, 054426 (2015).
- [33] P. Kuświk, P. L. Gastelois, M. M. Soares, H. C. N. Tolentino, M. De Santis, A. Y. Ramos, A. D. Lamirand, M. Przybylski, and J. Kirschner, *Phys. Rev. B* **91**, 134413 (2015).
- [34] M. T. Hutchings, *Phys. Rev. B* **6**, 3447 (1972).
- [35] W. Zhu, L. Seve, R. Sears, B. Sinkovic, and S. S. P. Parkin, *Phys. Rev. Lett.* **86**, 5389 (2001).
- [36] N. J. Gökeмейjer, J. W. Cai, and C. L. Chien, *Phys. Rev. B* **60**, 3033 (1999).
- [37] C. Kittel, *Phys. Rev.* **70**, 965 (1946).
- [38] Y. Yafet and E. M. Gyorgy, *Phys. Rev. B* **38**, 9145 (1988).
- [39] Y. Z. Wu, C. Won, A. Scholl, A. Doran, H. W. Zhao, X. F. Jin, and Z. Q. Qiu, *Phys. Rev. Lett.* **93**, 117205 (2004).